Molecular Plant
Research Article

CellPress
Partner Journal

Cell wall β-1,4-galactan regulated by the BPC1/BPC2-GALS1 module aggravates salt sensitivity in *Arabidopsis thaliana*

Jingwei Yan[1,2], Ya Liu[1], Lan Yang[1], Huan He[1], Yun Huang[1], Lin Fang[3], Henrik Vibe Scheller[4,5], Mingyi Jiang[1,2] and Aying Zhang[1,2,*]

[1]College of Life Sciences, Nanjing Agricultural University, Nanjing, Jiangsu 210095, China

[2]State Key Laboratory of Crop Genetics and Germplasm Enhancement, Nanjing Agricultural University, Nanjing, Jiangsu 210095, China

[3]Guangdong Provincial Key Laboratory of Applied Botany, South China Botanical Garden, Chinese Academy of Sciences, Guangzhou, Guangdong 510650, China

[4]Joint Bioenergy Institute and Environmental Genomics and Systems Biology Division, Lawrence Berkeley National Laboratory, Berkeley, CA 94720, USA

[5]Department of Plant and Microbial Biology, University of California, Berkeley, CA 94720, USA

***Correspondence: Aying Zhang (ayzhang@njau.edu.cn)**

https://doi.org/10.1016/j.molp.2020.11.023

ABSTRACT

Salinity severely reduces plant growth and limits agricultural productivity. Dynamic changes and rearrangement of the plant cell wall is an important response to salt stress, but relatively little is known about the biological importance of specific cell wall components in the response. Here, we demonstrate a specific function of β-1,4-galactan in salt hypersensitivity. We found that salt stress induces the accumulation of β-1,4-galactan in root cell walls by up regulating the expression of *GALACTAN SYNTHASE 1* (*GALS1*), which encodes a β-1,4-galactan synthase. The accumulation of β-1,4-galactan negatively affects salt tolerance. Exogenous application of D-galactose (D-Gal) causes an increase in β-1,4-galactan levels in the wild type and *GALS1* mutants, especially in *GALS1* overexpressors, which correlated with the aggravated salt hypersensitivity. Furthermore, we discovered that the BARLEY B RECOMBINANT/BASIC PENTACYSTEINE transcription factors BPC1/BPC2 positively regulate plant salt tolerance by repressing *GALS1* expression and β-1,4-galactan accumulation. Genetic analysis suggested that *GALS1* is genetically epistatic to *BPC1/BPC2* with respect to the control of salt sensitivity as well as accumulation of β-1,4-galactan. Taken together, our results reveal a new regulatory mechanism by which β-1,4-galactan regulated by the BPC1/BPC2-GALS1 module aggravates salt sensitivity in *Arabidopsis thaliana.*

Key words: salt stress, β-1,4-galactan, GALS1, BPC1/BPC2, *Arabidopsis thaliana*

Yan J., Liu Y., Yang L., He H., Huang Y., Fang L., Scheller H.V., Jiang M., and Zhang A. (2021). Cell wall β-1,4-galactan regulated by the BPC1/BPC2-GALS1 module aggravates salt sensitivity in *Arabidopsis thaliana*. Mol. Plant. **14**, 411–425.

INTRODUCTION

Salt stress is a major abiotic stress that severely reduces plant growth and limits agricultural productivity (Zhu, 2002, 2016). Plants have evolved various strategies to sense and adapt to saline environments (Munns and Tester, 2008; Julkowska and Testerink, 2015; Zhu, 2016). Cell walls provide the cell with both structural support and protection. One of the important plant adaptations to salt stress is differential regulation of growth, accompanying the dynamic changes and rearrangement of the plant cell wall (Cosgrove, 2015; Tenhaken, 2015; Wang et al., 2016). The plant cell wall has a dynamic architecture composed of cellulose microfibrils embedded in an amorphous matrix of pectin and hemicellulose polysaccharides as well as structural proteins, and in some cells also lignin (Mutwil et al., 2008; Scheller and Ulvskov, 2010; Herburger et al., 2020). Previous studies have shown that several cellulose synthesis genes, including *Cellulose Synthase* (*CesA1*, *CesA6*, and *CesA8*), *Cellulose Synthase-Like D5* (*CSLD5*), KORRIGAN1 (*KOR1*), and *Companion of Cellulose Synthase* (*CC1* and *CC2*), are implicated in salt stress (Chen et al., 2005; Kang et al., 2008; Zhu et al., 2010; Endler et al., 2015; Zhang et al., 2016; Liu et al., 2018; Kesten et al., 2019). Knocking out *CesA6* confers salt stress sensitivity (Zhang et al., 2016). CC1 and CC2 interact

Published by the Molecular Plant Shanghai Editorial Office in association with Cell Press, an imprint of Elsevier Inc., on behalf of CSPB and CEMPS, CAS.

with CesAs and microtubules, and mutations in *CC1* and *CC2* disrupt salt tolerance by altering microtubule and cellulose synthase complex properties (Endler et al., 2015; Kesten et al., 2019). Thus, sustained cellulose biosynthesis is crucial for plants to cope with salt stress.

β-1,4-Galactan are generally found as side chains of rhamnogalacturonan I, which is a major component of pectin (Harholt et al., 2010; Atmodjo et al., 2013). β-1,4-Galactan is directly synthesized by β-1,4-galactan galactosyltransferase encoded by *GALACTAN SYNTHASE* genes, of which there are three in *Arabidopsis thaliana* (*Arabidopsis*), *GALS1*, *GALS2*, and *GALS3* (Liwanag et al., 2012; Ebert et al., 2018). Several studies have shown that β-1,4-galactan plays a role in plant growth and development. For example, overexpressing a fungal galactanase in potato tubers resulted in decreased β-1,4-galactan and slightly altered mechanical properties (Ulvskov et al., 2005). Øbro et al. (2009) found that reduced β-1,4-galactan slightly affected the diameter of stems in *Arabidopsis*. In flax, β-1,4-galactan confers specific mechanical properties to cellulose-enriched plant fibers by modifying β-1,4-galactan metabolism *in muro* (Roach et al., 2011). β-1,4-Galactan might also play a role in cell elongation by altering the cell wall properties (McCartney et al., 2003; Moneo-Sánchez et al., 2019). Furthermore, β-1,4-galactan is believed to be a water-retaining viscoelastic component with a likely role in modulating the mechanical properties of the cell wall (Tang et al., 1999; Ha et al., 2005; Harholt et al., 2010). Nevertheless, even *Arabidopsis* triple mutants in all three *GALS* genes showed no observable growth or developmental phenotype under standard laboratory conditions (Ebert et al., 2018). However, given the conservation across plants of β-1,4-galactan it must serve an important role. Surprisingly, the involvement of β-1,4-galactan in plant response to abiotic stresses has not been reported.

The BARLEY B RECOMBINANT/BASIC PENTACYSTEINE (BBR/BPC) proteins comprise a plant-specific transcription factor family and are present throughout land plants. They have been identified in many species, including *Arabidopsis*, *Oryza sativa*, *Hordeum vulgare*, *Glycine max*, and *Cucumis sativus* (Kooiker et al., 2005; Monfared et al., 2011; Mu et al., 2017a; Mu et al., 2017b; Sangwan and O'Brian, 2002; Santi et al., 2003). BPC proteins containing a conserved DNA-binding domain at the C-terminal can directly regulate the expression of target genes by binding GA-rich sequences of promoters (Kooiker et al., 2005; Meister et al., 2004; Mu et al., 2017b; Sangwan and O'Brian, 2002; Santi et al., 2003; Simonini et al., 2012). In *Arabidopsis,* 7% of promoters contain at least one GA-rich sequence according to a pattern-matching search (Yan et al., 2005). This high frequency of sequence motif in the genome suggests that the BPC proteins might have numerous and distinct functions during plant growth. Indeed, BPC proteins regulate a wide range of developmental processes, including seed dormancy, inflorescence meristem, leaf and flower development, lateral root formation, and cytokinin response (Monfared et al., 2011; Simonini et al., 2012; Mu et al., 2017a, 2017b; Shanks et al., 2018; Wu et al., 2020). However, relatively little is known about the potential role of BPC proteins in abiotic stress responses.

In this study, we found that β-1,4-galactan significantly aggravated salt sensitivity in *Arabidopsis*. Furthermore, two transcription factors BPC1/BPC2 were found to directly bind the *GALS1* promoter, to repress *GALS1* expression, resulting in decreased β-1,4-galactan accumulation and increased salt tolerance.

RESULTS

Salt stress induces the accumulation of β-1,4-galactan in root cell wall

Salt stress inhibits primary root elongation (Galvan-Ampudia and Testerink, 2011). To investigate the potential role of the root cell wall in plant response to salt stress, we first determined the root cell wall composition in response to salt stress. Salt stress significantly increased the D-galactose (D-Gal) contents in the root cell wall, whereas the amount of other monosaccharide residues remained unchanged (Figure 1A).

Galactose is present in various polymers and glycoproteins in cell walls, including β-1,4-galactan and xyloglucan. To determine if the increase in D-Gal was related to increased β-1,4-galactan, cell wall material was digested with endo-β-1,4-galactanase from *Aspergillus niger* (Liwanag et al., 2012; Stonebloom et al., 2016), and the D-Gal content was analyzed in the solubilized and residual materials. Treatment with endo-β-1,4-galactanase released more D-Gal from the cell wall of salt-treated plants than from control plants, whereas the residual material did not show any difference (Figure 1B). This indicates that the increase in total D-Gal is specifically due to an increase in pectic β-1,4-galactan content.

The change in cell wall polysaccharides in response to salt stress was further investigated with immunodot assays using LM5 antibody, which specifically recognize pectic β-1,4-galactan (Jones et al., 1997). As shown in Figure 1C, binding was stronger in the material from the salt-treated plants than the control plants. Meanwhile, LM19, a monoclonal antibody against homogalacturonan (Verhertbruggen et al., 2009), did not show any difference in binding. The detection of the LM5 galactan epitope was strongly increased at the root tips of the salt-treated plants (Figure 1D), and the LM5 fluorescence intensity was enhanced significantly after salt stress (Figure 1E). These results show that salt stress induces the accumulation of β-1,4-galactan in the root cell wall.

GALS1 negatively affects plant salt stress tolerance

Previous studies have shown that three galactan synthase proteins (GALS1, GALS2, and GALS3) are involved in β-1,4-galactan biosynthesis (Liwanag et al., 2012; Ebert et al., 2018; Laursen et al., 2018). To investigate which *GALS* genes are involved in salt-induced accumulation of β-1,4-galactan in roots, the expression of *GALS1*, *GALS2*, and *GALS3* under NaCl treatment was examined. The expression of *GALS1* was strongly induced after 125 mM NaCl treatment, whereas salt stress did not affect the expression of *GALS2* and *GALS3* (Figure 2A–2C). Plants were transformed with a construct where the promoter region of *GALS1*, *GALS2*, or *GALS3* was fused to a β-glucuronidase (GUS) reporter gene. GUS activity was strongly detected in the root tip of transgenic lines with *Pro-GALS1-GUS* and more weakly observed in the root tip of transgenic lines with *Pro-GALS2-GUS* and *Pro-GALS3-GUS* (Figure 2D–2F). Salt stress only obviously increased the GUS activities in the root tip of *Pro-GALS1-GUS* lines (Figure 2D), consistent with the qRT–PCR results.

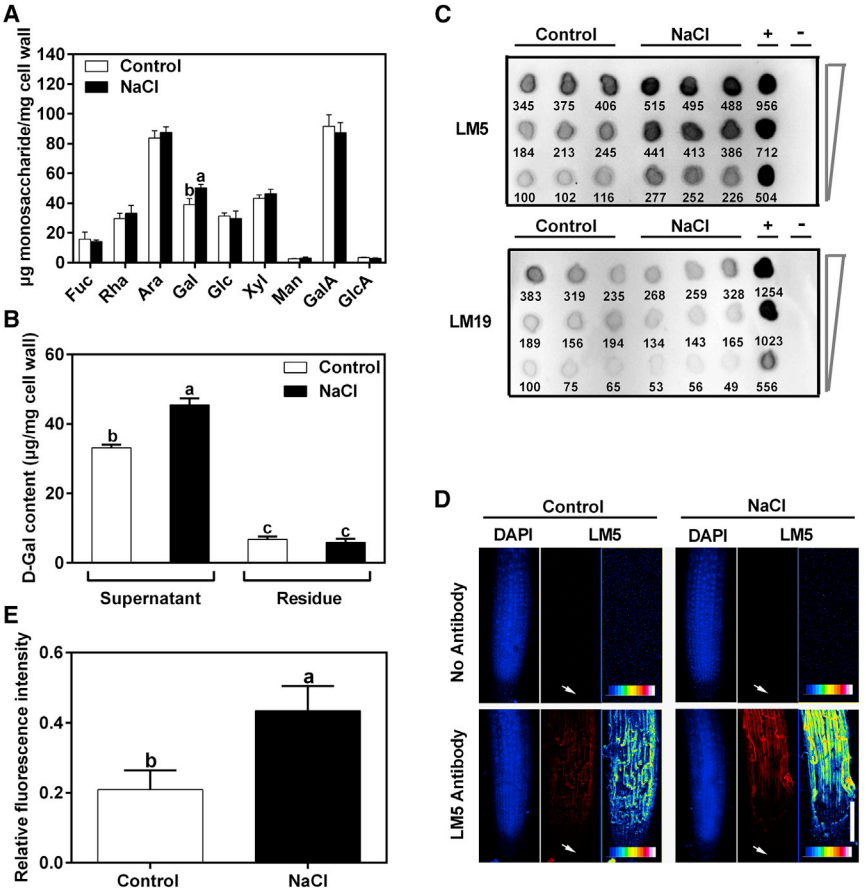

Figure 1. Salt stress induces the accumulation of β-1,4-galactan in root cell wall of *Arabidopsis*.

(A) Monosaccharide composition of root cell walls in wild-type plants exposed to salt stress. Four-day-old seedlings of Col-0 grown on 1/2 MS medium were transferred to 1/2 MS medium with or without 125 mM NaCl for 3 days. The AIR was extracted from roots, hydrolyzed with 2 M trifluoroacetic acid, and analyzed by HPAEC. Error bars in **(A)** represent SD (n = 3).

(B) AIR from roots after treatments indicated in **(A)** was digested with endo-β-1,4-galactanase, separated into supernatant and residue, and analyzed by HPEAC. Error bars in **(B)** represent SD (n = 3).

(C) Immunodot analysis of β-1,4-galactan in the root cell wall after treatments indicated in **(A)**. The blots were developed with the LM5 monoclonal antibody, which is specific for β-1,4-galactan, and the LM19 monoclonal antibody, which is specific for homogalacturonan. The triangles on the right indicate the dilutions of AIR spotted on the blots. Potato galactan (+) or sugar beet pectin (+) was used as positive control, and water (−) was used as a negative control. Relative intensities, normalized relative to the intensity with control in each nitrocellulose membrane (bottom left; this point was set to 100), are indicated by numbers below the points.

(D) Immunodetection of the β-1,4-galactan epitope in roots of wild type exposed to salt stress. Four-day-old seedlings of Col-0 grown on 1/2 MS medium were transferred to 1/2 MS medium with or without 125 mM NaCl for 3 days, then the confocal micrographs were obtained. DAPI (blue) was applied to stain the nucleus. The figure on the right side of each panel (LM5) is a pseudo-color image representing the fluorescence intensity. The color scales below the figures indicate the fluorescence intensity. Scale bar corresponds to 100 μm **(D)**. Arrows indicate the position of the root tip.

(E) Quantitative analysis of the relative fluorescence intensity of LM5 staining in the root tips as indicated in **(D)**. Error bars in **(E)** represent SD (n = 12). Different letters in **(A, B, and E)** indicate a significant difference compared with the control as determined by one-way ANOVA for $P < 0.05$.

To evaluate the contribution of GALS1 to root growth under NaCl treatment, two independent mutants of *GALS1* with T-DNA insertion (*gals1-1* and *gals1-2*) were used for salt sensitivity assays (Liwanag et al., 2012). Genotypes and decreased β-1,4-galactan in the mutants were confirmed by RT–PCR and immunodetection analysis (Supplemental Figure 1). Four-day-old seedlings of the wild type and *gals1* mutants were transferred to 1/2 Murashige and Skoog (MS) medium with or without 125 mM NaCl. No differences in primary root length were observed between wild type and *gals1* mutants grown on 1/2 MS medium without NaCl (Figure 2G). However, in the presence of NaCl, the primary root length of the *gals1* mutants was longer than those of the wild type (Figure 2G).

To further investigate the function of GALS1, we expressed *GALS1* driven by the native *GALS1* promoter in the *gals1-1* background and *GALS1* driven by the *35S* promoter in Col-0. As shown in Supplemental Figures 2 and 3, two independent complementation lines (*COM#1* and *COM#2*) and *GALS1* overexpressors (*OE-GALS1#1* and *OE-GALS1#5*) were confirmed by RT–PCR and immunodetection analysis. Under NaCl-free conditions, no differences in primary root growth were observed among the tested genotypes. Under NaCl treatment, the complemented lines did not differ from the wild type, whereas *GALS1* overexpressors showed a shorter primary root length (Figure 2H and 2I). Salt stress results in both osmotic and ionic stress in plant (Munns and Tester, 2008). Next, we determined whether salt tolerance of *gals1* mutants was a specific response to the sodium ions. As shown in Supplemental Figure 4, seedlings of *gals1-1* and *gals1-2* specifically responded to Na^+, but not K^+, Cl-, and osmotic stress. These results clearly indicate that GALS1 negatively affects salt tolerance.

β-1,4-galactan synthesized by *GALS1* significantly aggravates salt hypersensitivity in *Arabidopsis*

Our results showed that salt stress induced the accumulation of β-1,4-galactan in roots (Figure 1) and *GALS1* negatively affected the salt tolerance (Figure 2). The LM5 galactan epitope was significantly increased in the root tips of the wild type, *gals1* mutants, and the *GALS1* overexpressor under NaCl treatment. The LM5 fluorescence intensity in the *GALS1* overexpressor was much stronger than in the wild type, and LM5 signal in the *gals1* mutants was much weaker than in the wild type (Figure 3C and 3D). These findings are consistent with the observation that accumulation of β-1,4-galactan aggravates the stress symptoms induced by salt stress.

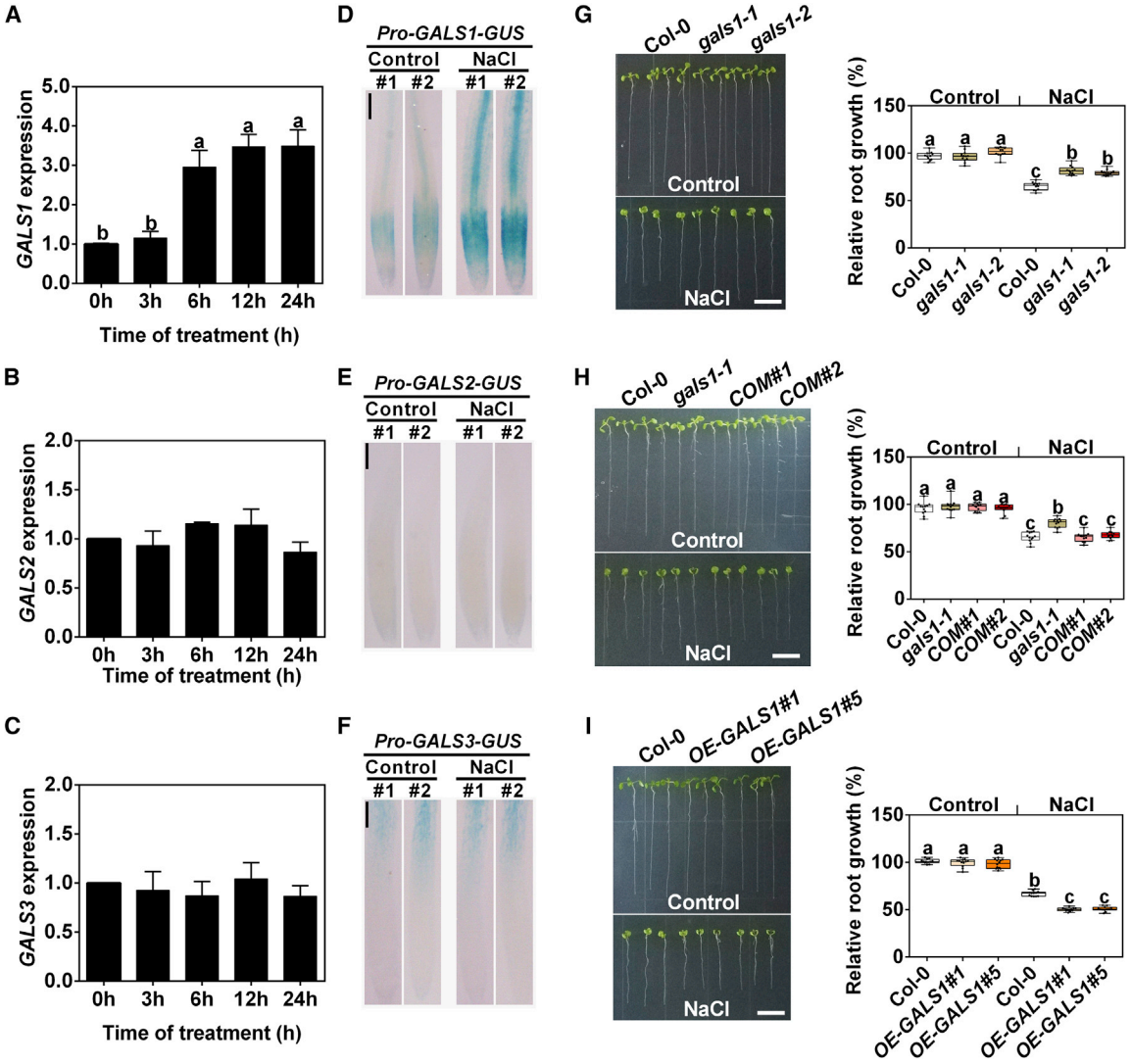

Figure 2. GALS1 negatively affects plant salt stress response.

(A–C) The expression of *GALS1*, *GALS2*, and *GALS3* in *Arabidopsis* roots exposed to salt stress. Four-day-old seedlings were treated with 125 mM NaCl for different times as indicated, before analysis of *GALS* expression in roots by qRT–PCR. Error bars in **(A–C)** represent SD ($n = 3$). Different letters in **(A–C)** indicate a significant difference compared with the control as determined by one-way ANOVA for $P < 0.05$.

(D–F) The expression patterns of *GUS* driven by *GALS* promoters under salt stress in roots. Seedlings were treated with 125 mM NaCl for 12 h and stained for GUS activity. Roots in **(D and F)** were stained for 3 h, and roots in **(E)** were stained for 24 h. Scale bars correspond to 100 μm **(D–F)**. Experiment in **(D–F)** were performed at least three times with similar results.

(G) Analysis of salt sensitivity in *–gals1* mutants. Four-day-old seedlings of *gals1-1*, *gals1-2*, and Col-0 grown on 1/2 MS medium were transferred to 1/2 MS medium with or without 125 mM NaCl. Photographs were taken after 7 days of treatment. Relative root length (percent of non-treated plants) was calculated.

(H) Analysis of salt sensitivity in complementation of *GALS1* in *gals1-1* (*COM#1* and *COM#2*). Four-day-old seedlings of *gals1-1*, complemented lines (*COM#1* and *COM#2*), and Col-0 grown on 1/2 MS medium were transferred to 1/2 MS medium with or without 125 mM NaCl. Photographs were taken after 7 days of treatment. Relative root length (percent of non-treated plants) was calculated.

(I) Analysis of salt sensitivity in *GALS1* overexpressors (*OE-GALS#1* and *OE-GALS1#5*). Four-day-old seedlings of *OE-GALS#1, OE-GALS1#5*, and Col-0 grown on 1/2 MS medium were transferred to 1/2 MS medium with or without 125 mM NaCl. Photographs were taken after 7 days of treatment. Relative root length (percent of non-treated plants) was calculated.

Scale bars correspond to 1 cm **(G–I)**. Standard boxplots ($n = 12$) are shown for **(G–I)**. Different letters in **(G–I)** indicate significant differences as determined by two-way ANOVA and Tukey's multiple comparisons test for $P < 0.05$.

Since D-Gal can be directly used by plants and exogenous D-Gal increased the D-Gal level but not other cell wall monosaccharides in etiolated hypocotyl cell walls (Laursen et al., 2018), a D-Gal-feeding experiment was conducted to explore the impact of exogenous D-Gal on the salt response (Dörmann and Benning, 1998; Seifert et al., 2002; Laursen et al., 2018). Our results showed that exogenous D-Gal significantly increased the accumulation of β-1,4-galactan in the roots of all tested genotypes (Figure 3C and 3D). To analyze the effect of exogenous D-Gal on salt sensitivity, 4-day-old seedlings of the wild type

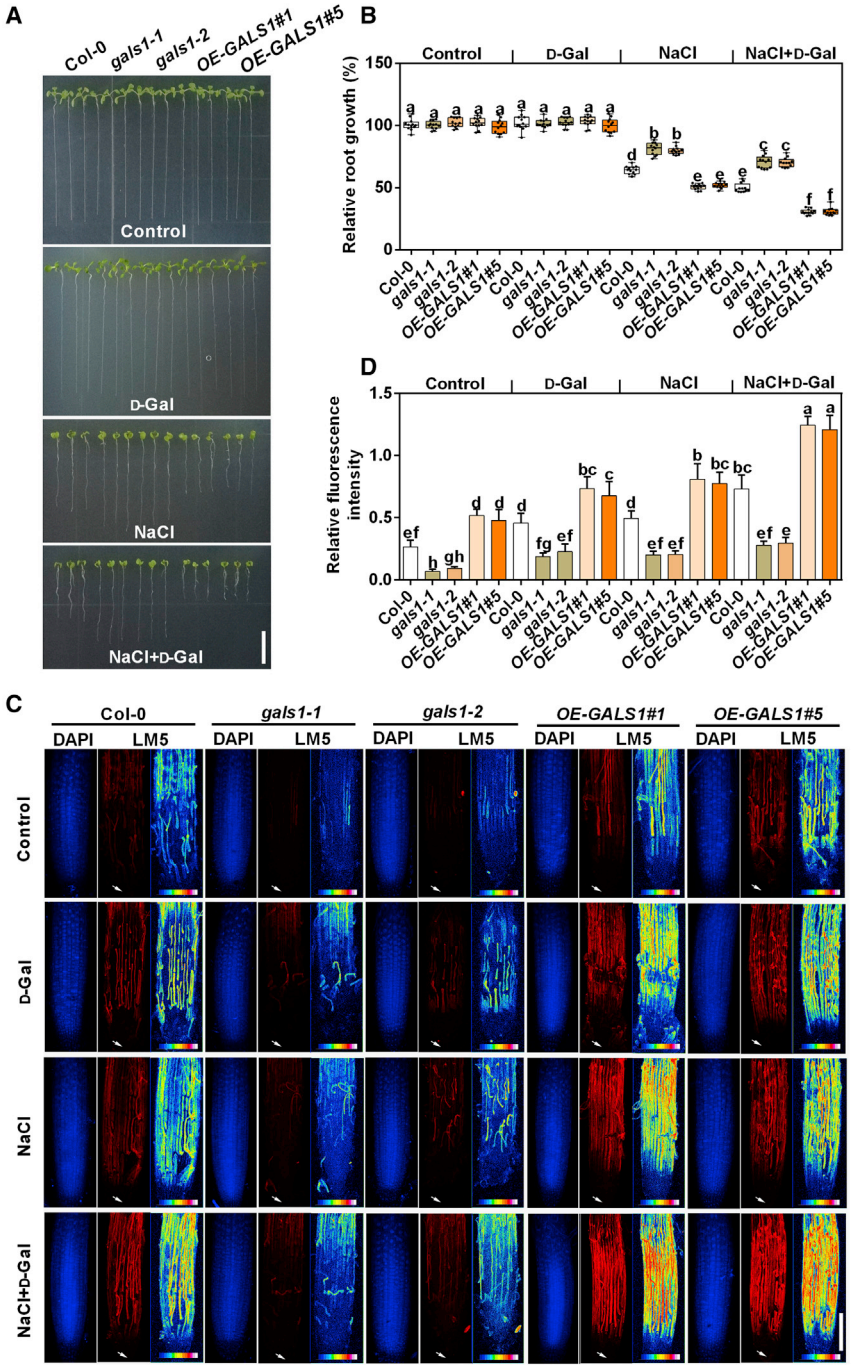

Figure 3. The accumulation of β-1,4-galactan plays a key role in salt hypersensitivity.

(A) Analysis of salt sensitivity in the *gals1* mutants and the *GALS1* overexpressors with or without D-galactose (D-Gal). Four-day-old seedlings of *gals1-1*, *gals1-2*, *OE-GALS1#1*, *OE-GALS1#5*, and Col-0 grown on 1/2 MS medium were transferred to 1/2 MS medium containing 0 or 25 mM D-galactose (D-Gal) and 0 or 125 mM NaCl. Photographs were taken after 7 days of treatment. Scale bar corresponds to 1 cm.

(B) Relative root length (percent of non-treated plants) tested in **(A)** is shown in standard boxplots (n = 12).

(C) Immunodetection of the β-1,4-galactan epitope in roots of wild type, *gals1* mutants, and *GALS1* overexpressors exposed to salt stress and exogenous D-galactose (D-Gal). Four-day-old seedlings of *gals1-1*, *gals1-2*, *OE-GALS1#1*, *OE-GALS1#5*, and Col-0 grown on 1/2 MS medium were transferred to 1/2 MS medium containing 0 or 25 mM D-galactose (D-Gal) and 0 or 125 mM NaCl for 3 days, then the confocal micrographs were obtained. DAPI (blue) was applied to stain the nucleus. The figure on the right side of each panel (LM5) is a pseudo-color image representing the fluorescence intensity. The color scales below the figures indicate the fluorescence intensity. Scale bar corresponds to 100 μm **(C)**. Arrows indicate the position of the root tip.

(D) Quantitative analysis of the relative fluorescence intensity of LM5 staining in the root tips as indicated in **(C)**. Error bars in **(D)** represent SD (n = 12). Different letters in **(B and D)** indicate significant differences as determined by two-way ANOVA and Tukey's multiple comparisons test for $P < 0.05$.

were transferred to 1/2 MS medium supplemented with or without 125 mM NaCl and various concentrations of D-Gal (0, 12.5 and 25 mM). In the absence of NaCl, exogenous D-Gal had no obvious effect on primary root growth. When seedlings grew on 1/2 MS medium supplemented with 125 mM NaCl, the presence of exogenous D-Gal significantly inhibited the primary root growth in a concentration-dependent manner. In contrast, supplementation with exogenous D-glucose (D-Glc), did not affect salt sensitivity (Supplemental Figure 5).

Next, we observed the effect of exogenous D-Gal on suppressing the primary root growth of *gals1* mutants and *GALS1* overexpressors. We found that exogenous application of D-Gal suppressed the primary root growth of all the genotypes in the presence of NaCl. Suppression of primary root length in the wild type was weaker than in the *GALS1* overexpressors, and stronger than in the *gals1* mutants (Figure 3A and 3B). Meanwhile, we determined the prevalence of the β-1,4-galactan epitope in the roots of the above tested genotypes. The induction of β-1,4-galactan levels correlated with the suppression of primary root growth in the wild type, *GALS1* overexpressors, and *gals1* mutants (Figure 3C and 3D). These results further confirm the strong correlation between β-1,4-galactan and salt sensitivity.

GALS1 affects crystalline cellulose biosynthesis under salt stress

Ebert et al. (2018) found that loss or accumulation of β-1,4-galactan led to minor changes in cellulose synthesis in *Arabidopsis* seedlings under normal condition. To explore whether cellulose contents were also affected in the *gals1* mutant and the *GALS1* overexpressor under NaCl treatment, the fluorescence of cellulose stained with Pontamine Fast Scarlet 4B (S4B) in roots

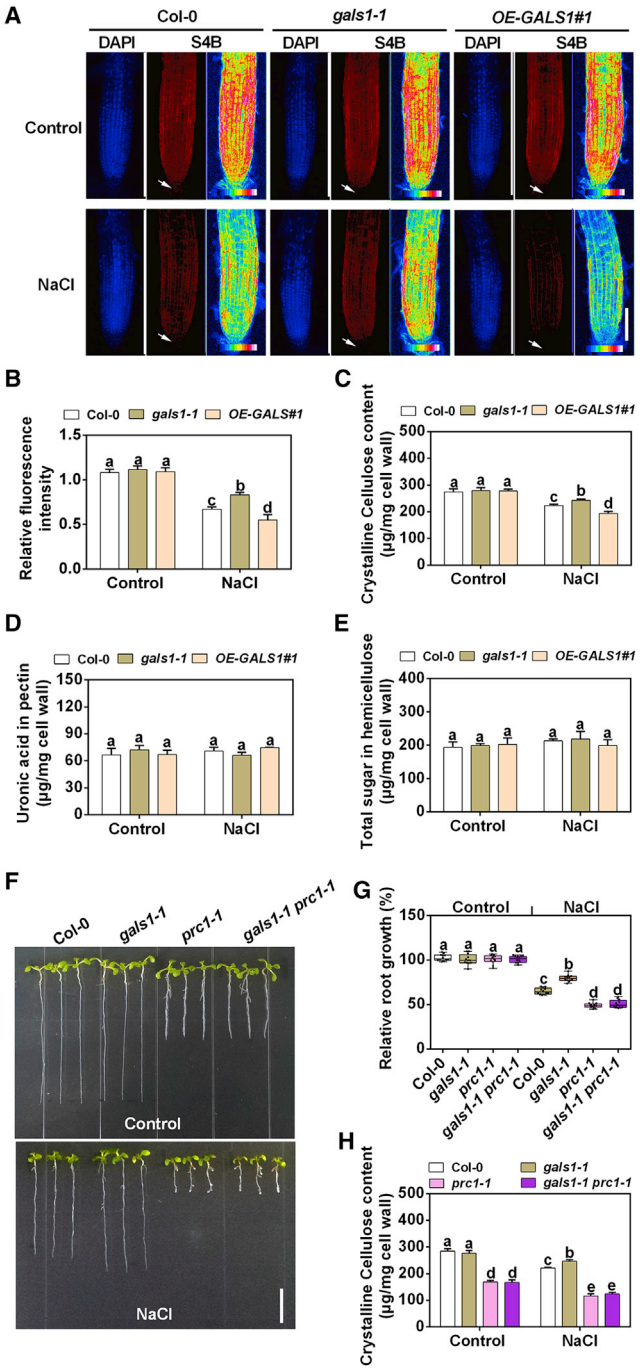

Figure 4. GALS1 affects crystalline cellulose biosynthesis under salt stress.

(A) Confocal imaging of S4B-stained root tips. Four-day-old seedlings of *gals1-1*, *OE-GALS#1*, and Col-0 grown on 1/2 MS medium were transferred to 1/2 MS medium with or without 125 mM NaCl for 3 days, then the confocal micrographs were obtained. DAPI (blue) was applied to stain the nucleus. The figure on the right side of each panel (S4B) is a pseudo-color image representing the fluorescence intensity. The color scales below the figures indicate the fluorescence intensity. Scale bar corresponds to 100 μm **(A)**. Arrows indicate the position of the root tip.

(B) Quantitative analysis of the relative fluorescence intensity of S4B staining in the root tips as indicated in **(A)**. Error bars in **(B)** represent SD (n = 12).

from the tested genotypes was determined (Anderson et al., 2010). As shown in Figure 4A and 4B, the cellulose fluorescence intensity in the root of the wild type was stronger than that of the *OE-GALS1#1* overexpressor, but lower than that of the *gals1-1* mutant under NaCl treatment. To confirm this, we then analyzed the crystalline cellulose content in the root cell wall of these genotypes under NaCl treatment. In the presence of NaCl, the crystalline cellulose content in the *gals1-1* root was higher compared with that of the wild type, while the crystalline cellulose content in *OE-GALS1#1* was lower compared with that of the wild type (Figure 4C). However, there was no significant difference in D-Glc content in trifluoroacetic acid (TFA)-hydrolyzate between the *gals1* mutant and the *GALS1* overexpressor under NaCl treatment, suggesting that GALS1 did not affect the amorphous cellulose content in response to salt stress (Supplemental Table 1).

To further investigate whether GALS1 affects other cell wall components in response to salt stress, we measured the contents of pectin and hemicellulose in salt-treated roots of *gals1-1*, *OE-GALS1#1*, and Col-0. In the absence or presence of NaCl, the contents of pectin and hemicellulose in the *gals1* mutants and the *GALS1* overexpressors were similar to those in the wild type (Figure 4D and 4E). Monosaccharide composition analysis showed that only the D-Gal contents in the root cell wall were affected in the *gals1* mutant and the *GALS1* overexpressor under NaCl treatment (Supplemental Table 1). Together, these results indicate that GALS1 negatively affects crystalline cellulose synthesis only under salt stress.

To further confirm the effect on crystalline cellulose, the *prc1-1* mutant (a knockout mutant of *CesA6*) with a defect in crystalline cellulose synthesis (Fagard et al., 2000) was crossed with the *gals1-1* mutant. The *prc1-1* mutant was highly sensitive to salt stress compared with the wild type (Supplemental Figure 6) as previously reported (Zhang et al., 2016). The *gals1-1 prc1-1* double mutant was confirmed by PCR and Sanger sequence (Supplemental Figure 7). As shown in Figure 4F and 4G, the primary root growth of the *gals1-1 prc1-1* double mutant was similar to that of the *prc1-1* single mutant under both normal

(C–E) The crystalline cellulose content, pectin content, and hemicellulose content in the root cell wall from *gals1-1*, *OE-GALS#1*, and wild type in response to salt stress. Four-day-old seedlings of *gals1-1*, *OE-GALS#1*, and Col-0 grown on 1/2 MS medium were transferred to 1/2 MS medium with or without 125 mM NaCl for 3 days. Error bars in **(C–E)** represent SD (n = 3).

(F) The salt tolerance of *gals1-1* mutant is abolished by suppression of *CESA6*. Four-day-old seedlings of *gals1-1*, *prc1-1* (*CESA6* mutant), *gals1-1 prc1-1*, and Col-0 grown on 1/2 MS medium were transferred to 1/2 MS medium with or without 125 mM NaCl. Photographs were taken after 7 days of treatment. Scale bar corresponds to 1 cm **(F)**.

(G) Relative root length (percent of non-treated plants) tested in **(F)** is shown in standard boxplots (n = 12).

(H) The crystalline cellulose content in the root cell wall from *gals1-1*, *prc1-1*, *gals1-1 prc1-1*, and wild type in response to salt stress. Four-day-old seedlings of *gals1-1*, *prc1-1*, *gals1-1 prc1-1*, and Col-0 grown on 1/2 MS medium were transferred to 1/2 MS medium with or without 125 mM NaCl for 3 days. Error bars in **(H)** represent SD (n = 3).

Different letters in **(B–E, G, and H)** indicate significant differences as determined by two-way ANOVA and Tukey's multiple comparisons test for $P < 0.05$.

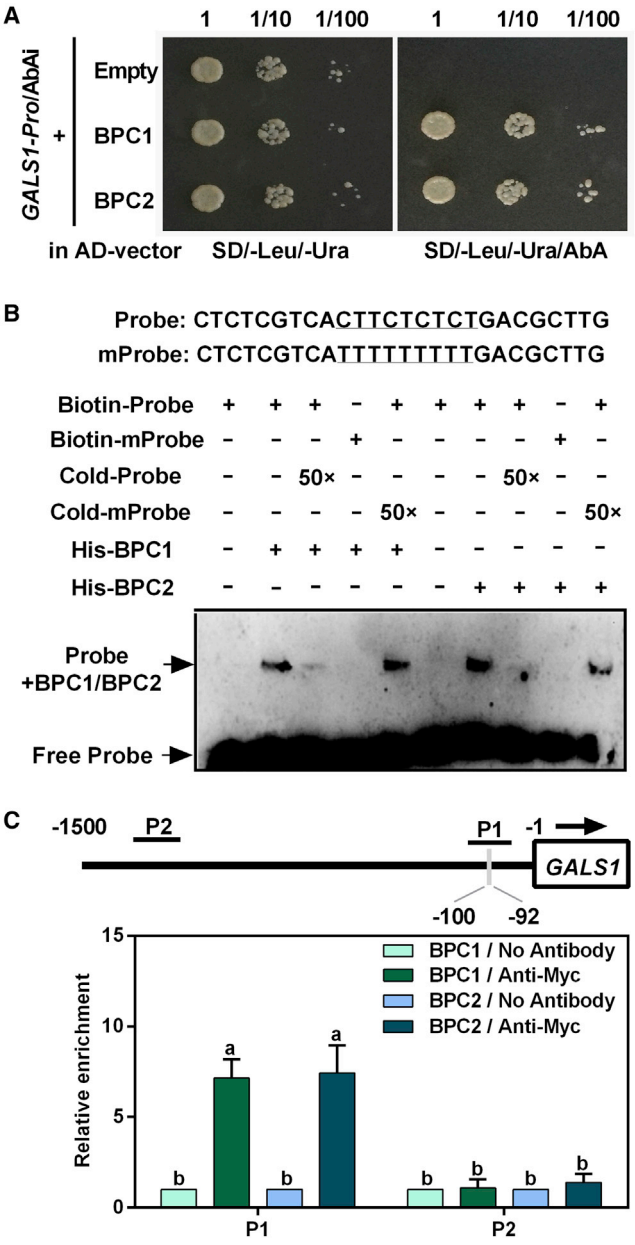

Figure 5. BPC1/BPC2 directly bind the promoter of *GALS1* *in vitro* and *in vivo*.

(A) BPC1 or BPC2 binds the *GALS1* promoter in yeast. Y1HGold strain co-transformed *GALS1-promoter* linked to the *Aureobasidin 1-C* (AbA^r) (*GALS1-Pro*/AbAi) and pGADT7 AD-BPC1 (BPC1-AD), pGADT7 AD-BPC2 (BPC2-AD), or pGADT7 AD vector alone (AD) was grown on the SD/-Leu/-Ura with or without 300 ng/ml AbA for 3 days. Number at the top represents the dilutions times of an optical density at 600 nm.

(B) BPC1 or BPC2 binds to the *GALS1* promoter via EMSA assay. Purified protein was incubated with a biotin-labeled Probe (Biotin-Probe) and a control biotin-labeled mProbe (Biotin-mProbe). For the competition test, a non-labeled probe (Cold-Probe) with excess (50 times) or non-labeled mProbe (Cold-mProbe) was added in the above experiment.

(C) BPC1 or BPC2 interacts with the *GALS1* promoter via a ChIP–qPCR assay. The upstream region is a schematic representation of putative BPC binding sites in the regions 1500 bp upstream of the start site in the *GALS1* promoter. Gray lines indicate the CTTCTCTCT motif (−92 to −100). P1 and P2 represent the fragments amplified in the ChIP assay. Chromatin was isolated from 10-day-old *Arabidopsis* seedlings of *Pro-BPC1-BPC1-Myc* (BPC1) or *Pro-BPC2-BPC2-Myc* (BPC2) plants. Chromatin was immunoprecipitated with Myc antibody produced in mice (anti-Myc, Sigma-Aldrich). The measured values in control (no antibody) were set to 1 after normalization against *ACTIN 2* for quantitative PCT analysis. The experiment in **(A and B)** was performed at least three times with similar results. Values in **(C)** show average ± SD ($n = 3$). Different letters in **(C)** indicate a significant difference compared with the control as determined by one-way ANOVA for $P < 0.05$.

and NaCl conditions, even though the *gals1-1* single mutant showed a salt-resistant phenotype. The crystalline cellulose level in the *gals1-1 prc1-1* double mutant was also as low as that of the *prc1-1* single mutant, even though the *gals1-1* single mutant showed a high crystalline cellulose level (Figure 4H). The epistasis of *prc1-1* over *gals1-1* indicates that the sustained crystalline cellulose biosynthesis is responsible for the salt-resistant phenotype in the *gals1-1* mutant.

BPC1/BPC2 directly binds the promoter of *GALS1 in vivo* and *in vitro*

To investigate the regulation of the expression of *GALS1* under salt stress, we constructed three 5′ terminal deletion mutants of the *GALS1* promoter fused with the reporter gene *Firefly Luciferase* (*FFluc*) to transform into Col-0 (Supplemental Figure 8A). Seedlings of these *Arabidopsis* transgenic lines (*Pro-GALS1-FFluc*) were used to test the *GALS1* promoter activity under the NaCl treatment. As shown in Supplemental Figure 8B, the luminescence signal in NaCl-treated seedlings was significantly stronger than that in control plants. Importantly, there was no significant difference between *Pro-GALS1-FFluc* (1–600) and the other transgenic lines, which clearly demonstrated that the 1–600 bp fragment of the *GALS1* promoter retained the *GALS1* promoter activity and inducibility in response to salt stress.

To identify the putative transcription factors regulating *GALS1* expression, we constructed an *Arabidopsis* cDNA library and applied a yeast one-hybrid (Y1H) approach to search for novel transcription factors associated with the *GALS1* promoter. By determining the minimal inhibitory concentration of aureobasidin A (AbA) that suppressed background activation, we found that the fragment of *GALS1* promoter (1–600 bp) could not be directly used for this Y1H system because it was likely being recognized by endogenous yeast transcription factors (Supplemental Figure 9). Then, a series of deletion constructions of the *GALS1* promoter, as shown in Supplemental Figure 9, was used to test the minimal inhibitory concentration of AbA. We found that a slightly shorter fragment of the *GALS1* promoter (90–600 bp) could be used to screen the *Arabidopsis* cDNA library (Supplemental Figure 9). Positive interactions are listed in Supplemental Table 2. Two of the 16 positive clones encoded a BPC transcription factor, BPC1 (AT2G01930), and three of the 16 positive clones encoded a BPC transcription factor, BPC2 (AT1G14685).

To confirm the interactions between the *GALS1* promoter and the BPC1/BPC2 transcription factors, we performed the Y1H assay a second time using the full-length coding sequences of *BPC1* and *BPC2*. The interaction between BPC1/BPC2 and a fragment (90–600 bp) of the *GALS1* promoter was tested by growing on medium lacking Leu and Ura and supplemented with 300 ng/ml AbA. The assay showed that BPC1/BPC2 could bind to the promoter of *GALS1* in yeast (Figure 5A). In *Arabidopsis*, seven BPC

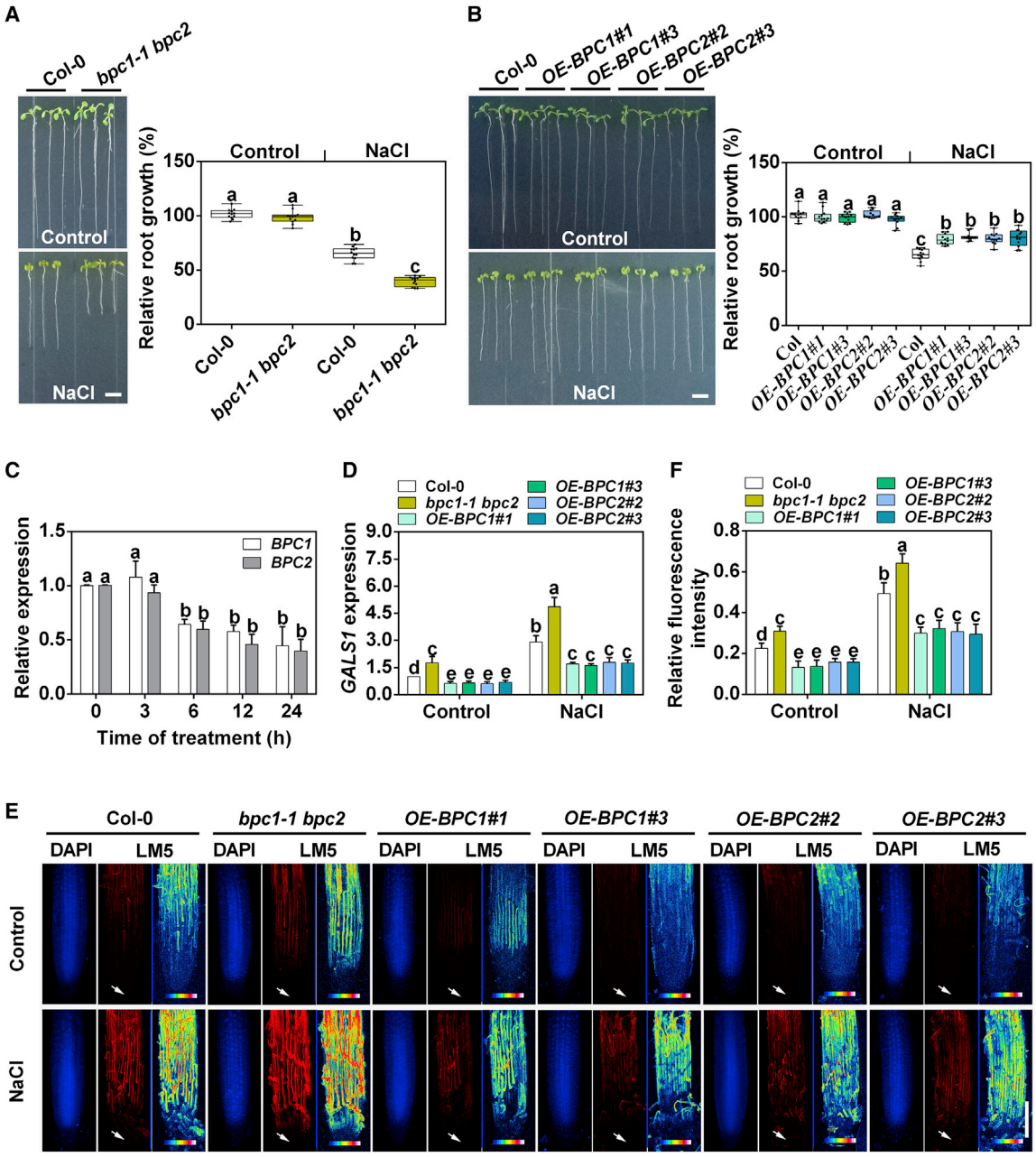

Figure 6. BPC1/BPC2 positively regulate plant salt tolerance by repressing *GALS1* expression to modulate the β-1,4-galactan accumulation in *Arabidopsis* roots.

(A) Analysis of salt sensitivity in *bpc1-1 bpc2* mutants. Four-day-old seedlings of *bpc1-1 bpc2* and Col-0 grown on 1/2 MS medium were transferred to 1/2 MS medium with or without 125 mM NaCl. Photographs were taken after 7 days of treatment. Relative root length (percent of non-treated plants) was calculated.

(B) Analysis of salt sensitivity in *BPC1* overexpressors (*OE-BPC1#1* and *OE-BPC1#3*) and *BPC2* overexpressors (*OE-BPC2#2* and *OE-BPC2#3*). Four-day-old seedlings of the above overexpressors and Col-0 grown on 1/2 MS medium were transferred to 1/2 MS medium with or without 125 mM NaCl. Photographs were taken after 7 days of treatment. Relative root length (percent of non-treated plants) was calculated. Scale bars correspond to 5 mm **(A and B)**. Standard boxplots (n = 12) are shown for **(A and B)**.

(C) The *BPC1* and *BPC2* expression in *Arabidopsis* roots exposed to salt stress. Four-day-old seedlings were treated with 125 mM NaCl for different times as indicated, then the *BPC1* and *BPC2* expression in roots were analyzed by qRT–PCR. Error bars in **(C)** represent SD (n = 3).

(D) The expression of *GALS1* in *Arabidopsis* roots from the above overexpressors, *bpc1-1 bpc2* mutant, and Col-0 exposed to salt stress. Four-day-old seedlings of the above genotypes were treated with 125 mM NaCl for 12 h, then the *GALS1* expression in roots was analyzed by qRT–PCR. Error bars in **(D)** represent SD (n = 5).

(E) Immunodetection of the β-1,4-galactan epitope in roots of the above genotypes exposed to salt stress. Four-day-old seedlings of the above genotypes grown on 1/2 MS medium were transferred to 1/2 MS medium with or without 125 mM NaCl for 3 days, then the confocal micrographs were

(legend continued on next page)

proteins are classified into three groups; BPC1, BPC2, and BPC3 are designated as class I (Monfared et al., 2011). However, we found that BPC3 could not directly bind to the *GALS1* promoter in yeast (Supplemental Figure 10).

BPC proteins can bind to sequences rich in GA repeats (Kooiker et al., 2005; Meister et al., 2004; Mu et al., 2017b; Sangwan and O'Brian, 2002; Santi et al., 2003; Simonini et al., 2012). We then searched the putative BPC protein binding elements in the sequences 600 bp upstream of the coding region of *GALS1* and identified one GA-rich motif (−92 to −100) in the promoter region of *GALS1* (Figure 5C). To determine whether BPC1/BPC2 binds this GA-rich motif, an electrophoresis mobility shift assay (EMSA) was performed. His-BPC1 or His-BPC2 was expressed in *Escherichia coli* BL21 and purified from the soluble fraction. BPC1/BPC2 directly bound to the probes labeled with biotin, whereas BPC1/BPC2 could not bind to the mutated probes labeled with biotin. In addition, the binding activity between BPC1/BPC2 and the probe was almost abolished by the addition of unlabeled competitive probes (Figure 5B).

To determine whether BPC1/BPC2 directly binds to the promoter of *GALS1 in vivo*, a chromatin immunoprecipitation (ChIP) assay using *Pro-BPC1-BPC1-Myc* and *Pro-BPC2-BPC2-Myc* plants was performed. The ChIP–qPCR assay showed that BPC1/BPC2 protein could strongly bind to the P1 but not the P2 region of the promoter, which does not have a GA-rich motif (Figure 5C). Taken together, our results clearly suggest that BPC1/BPC2 directly binds to the *GALS1* promoter *in vitro* and *in vivo*.

BPC1/BPC2 positively regulate plant salt tolerance by repressing *GALS1* expression

Since BPC1/BPC2 could directly bind to the *GALS1* promoter *in vivo* and *in vitro* (Figure 5), we wanted to test whether BPC1/BPC2 is involved in plant response to salt stress. Two T-DNA insertion lines (*bpc1-1* and *bpc2*) (Monfared et al., 2011) were used for salt sensitivity assays. Four-day-old seedlings of the wild type, *bpc1-1*, and *bpc2* mutants were transferred to 1/2 MS medium with or without 125 mM NaCl. Unexpectedly, there were no obvious differences in primary root length between wild type and *bpc1-1* or *bpc2* mutants in the presence of NaCl (Supplemental Figure 11). Monfared et al. (2011) showed that there was a high level of redundancy among the *BPC* genes in *Arabidopsis* development and growth. Thus, we hypothesized a functional redundancy of *BPC1* or *BPC2* gene in plant response to salt stress. To test our hypothesis, we obtained the *bpc1-1 bpc2* double mutant (Monfared et al., 2011). As shown in Figure 6A and Supplemental Figure 11, the primary root length of the *bpc1-1 bpc2* double mutant was shorter than that in the wild type. To further investigate the function of BPC1/BPC2, two independent *BPC1* overexpressor lines (*OE-BPC1#1* and *OE-BPC1#3*) and two independent *BPC2* overexpressor lines (*OE-BPC2#2* and *OE-BPC2#3*) were confirmed by qRT–PCR (Supplemental Figure 12) and investigated in salt sensitivity assays. Under NaCl-free conditions, no differences in primary root growth were observed among the tested genotypes. Under NaCl treatment, compared with the wild type, *BPC1* overexpressors and *BPC2* overexpressors showed a longer primary root length (Figure 6B). Moreover, we analyzed the *BPC1* and *BPC2* expression in response to salt stress and found that salt stress significantly reduced the expression of both genes (Figure 6C). These results clearly suggest that BPC1/BPC2 positively regulates salt tolerance.

To further test whether BPC1/BPC2 directly regulates *GALS1* expression, we quantified the expression of *GALS1* in the *bpc1-1 bpc2* double mutant, the *BPC1* overexpressors, and the *BPC2* overexpressors with or without NaCl treatment. The transcript of *GALS1* was markedly increased in the *bpc1-1 bpc2* double mutant, while *GALS1* expression was repressed in *BPC1* overexpressors and *BPC2* overexpressors both in the absence and presence of NaCl (Figure 6D). Furthermore, we analyzed the β-1,4-galactan levels in these genotypes. In agreement with *GALS1* expression, the β-1,4-galactan level was increased in the *bpc1-1 bpc2* double mutant, while it was significantly suppressed in *BPC1* and *BPC2* overexpressors (Figure 6E and 6F). These results demonstrate that BPC1/BPC2 positively affects the salt tolerance by repressing *GALS1* expression to modulate β-1,4-galactan accumulation.

To further determine the number of other genes regulated by BPC1/BPC2 proteins in response to salt stress, an RNA sequencing assay for both the wild type and the *bpc1-1 bpc2* mutant exposed to salt stress was performed. The RNA sequencing data showed that 1838 genes were upregulated, and that 1646 genes were downregulated in the wild type after NaCl treatment. In the *bpc1-1 bpc2* double mutant, 1839 genes were upregulated and 1422 genes were downregulated after NaCl treatment (Supplemental Figure 13A). Subsequent comparisons identified 629 genes (365 activated genes and 264 repressed genes) that were differentially expressed in NaCl-treated *bpc1-1 bpc2* mutant roots compared with NaCl-treated wild type roots (Supplemental Figure 13B and Supplemental Data 1). According to a gene ontology analysis the 629 BPC1/BPC2-dependent differentially expressed genes in response to NaCl treatment could be classified into a diverse range of categories: 182 genes (28.9%) in response to stimulus, 334 genes (53.1%) in cellular processes, 15 genes (2.4%) associated with growth, 11 genes (1.7%) in immune system processes, and so on (Supplemental Figure 13C and Supplemental Data 1). Therefore, these results reveal that BPC1/BPC2 have a significant impact on the global gene expression profile under salt stress.

obtained. DAPI (blue) was applied to stain the nucleus. The figure on the right side of each panel (LM5) is a pseudo-color image representing the fluorescence intensity. The color scales below the figures indicate the fluorescence intensity. Scale bar corresponds to 100 μm **(E)**. Arrows indicate the position of the root tip.**(F)** Quantitative analysis of the relative fluorescence intensity of LM5 staining in the root tips as indicated in **(E)**. Error bar in **(F)** represents SD (n = 12). Different letters in **(C)** indicate a significant difference compared with the control as determined by one-way ANOVA for $P < 0.05$. Different letters in **(A, B, D, and F)** indicate significant differences as determined by two-way ANOVA and Tukey's multiple comparisons test for $P < 0.05$.

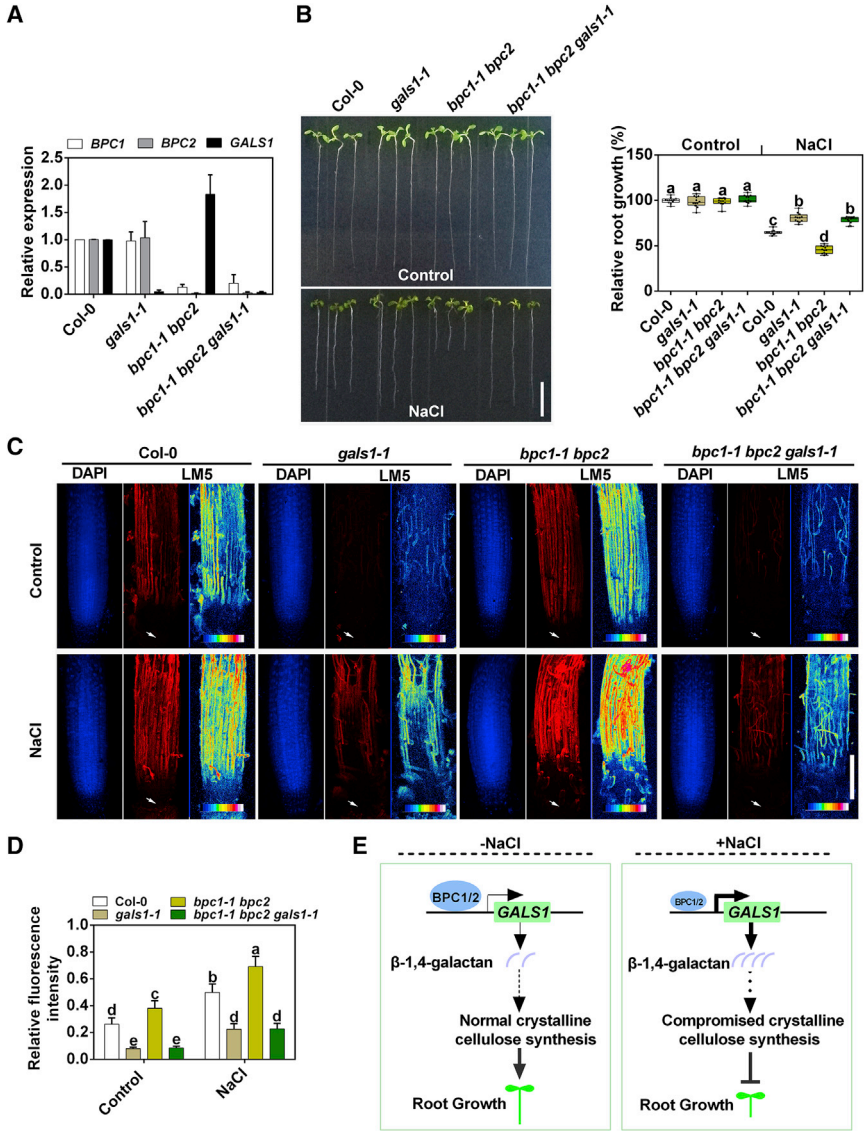

Figure 7. Genetic analysis of *bpc1-1 bpc2* with *gals1-1*.

(A) The expression of *BPC1*, *BPC2*, and *GALS1* in *Arabidopsis* roots from wild type, *gals1-1*, *bpc1-1 bpc2*, and *bpc1-1 bpc2 gals1-1* mutants. Error bars in **(A)** represent SD (n = 3).

(B) Analysis of salt sensitivity in wild type, *gals1-1*, *bpc1-1 bpc2*, and *bpc1-1 bpc2 gals1-1* mutants. Four-day-old seedlings of the above genotypes grown on 1/2 MS medium were transferred to 1/2 MS medium with or without 125 mM NaCl. Photographs were taken after 7 days of treatment. Scale bar corresponds to 1 cm **(B)**. Relative root length (percent of non-treated plants) was calculated. Standard boxplots (n = 12) are shown for **(B)**.

(C) Immunodetection of the β-1,4-galactan epitope in roots of wild type, *gals1-1*, *bpc1-1 bpc2*, and *bpc1-1 bpc2 gals1-1* mutants exposed to salt stress. Four-day-old seedlings of the above genotypes grown on 1/2 MS medium were transferred to 1/2 MS medium with or without 125 mM NaCl for 3 days, then the confocal micrographs were obtained. DAPI (blue) was applied to stain the nucleus. The figure on the right side of each panel (LM5) is a pseudo-color image representing the fluorescence intensity. The color scales below the figures indicate the fluorescence intensity. Scale bar corresponds to 100 μm **(C)**. Arrows indicate the position of the root tip.

(D) Quantitative analysis of the relative fluorescence intensity of LM5 staining in the root tips as indicated in **(C)**. Error bars in **(D)** represent SD (n = 12). **(E)** Proposed model that β-1,4-galactan regulated by BPC1/BPC2-GALS1 module aggravates salt sensitivity in *Arabidopsis*. Different letters in **(B and D)** indicate significant differences as determined by two-way ANOVA and Tukey's multiple comparisons test for $P < 0.05$.

GALS1 is epistatic to *BPC1/BPC2*

Our results indicate that the BPC1/BPC2-GALS1 transcriptional cascade is crucial for salt sensitivity by accumulating β-1,4-galactan in *Arabidopsis* roots. To confirm the genetic relationship between BPC1/BPC2 and GALS1, we crossed the *bpc1-1 bpc2* double mutant to the *gals1-1* single mutant to obtain the *bpc1-1 bpc2 gals1-1* triple mutant (Supplemental Figure 14). The transcripts of *BPC1, BPC2*, and *GALS1* were all disrupted in the *bpc1-1 bpc2 gals1-1* triple mutant (Figure 7A).

Next, we investigated the salt sensitivity of wild type, *gals1-1*, *bpc1-1 bpc2*, and *bpc1-1 bpc2 gals1-1* mutants. As shown in Figure 7B, the primary root growth of the *bpc1-1 bpc2 gals1-1* triple mutant was comparable with that of the *gals1-1* single mutant under NaCl treatment, indicating that BPC1/BPC2 is an upstream regulator of *GALS1* and that both genes act in the same pathway. After detecting the β-1,4-galactan fluorescence in different genotypes, we found that the β-1,4-galactan level in the *bpc1-1 bpc2 gals1-1* triple mutant was also as low as that in the *gals1-1* single mutant, even though the *bpc1-1 bpc2* double mutant showed a high level of β-1,4-galactan (Figure 7C and 7D). Therefore, we conclude that *GALS1* is genetically epistatic to *BPC1/BPC2* with respect to the control of salt sensitivity as well as accumulation of β-1,4-galactan in the root.

DISCUSSION

β-1,4-Galactan is one of the major cell wall polysaccharides and generally found as a side chain of rhamnogalacturonan I. A few studies have shown that β-1,4-galactan plays a role in plant growth and development (McCartney et al., 2003; Ulvskov et al., 2005; Øbro et al., 2009; Harholt et al., 2010; Roach et al., 2011; Moneo-Sánchez et al., 2019). However, *Arabidopsis* mutants essentially devoid of β-1,4-galactan show surprisingly normal growth and development (Ebert et al., 2018), suggesting that the important function of this polysaccharide would be more obvious under specific growth conditions, e.g., abiotic stress conditions. Here, we demonstrated a specific function of β-1,4-galactan in salt hypersensitivity.

Based on the modulation of β-1,4-galactan occurrence by growth inhibitors in *Arabidopsis* roots, McCartney et al. (2003) proposed a hypothesis that β-1,4-galactan might function in cell elongation. A recent study found that β-1,4-galactan turnover occurred during cell elongation in *Arabidopsis* etiolated hypocotyls and floral stem internodes (Moneo-Sánchez et al., 2019). These studies could suggest a link between the amount of β-1,4-galactan and root elongation in response to salt stress. In this study, we found that salt stress resulted in an increase in the amounts of β-1,4-galactan detected in the root tip of *Arabidopsis* (Figure 1). Epitope detection in immunofluorescence microscopy can be affected by masking by other polymers (Verhertbruggen et al., 2017). However, the detection of the LM5 epitope, the sugar composition analyses of root cell walls, and the *GALS1* expression levels, were always correlated, and we did not see evidence of a change in other pectic polysaccharides that could have affected masking effects. To date, three GALACTAN SYNTHASE genes, GALS1, GALS2, and GALS3, were reported to synthesize β-1,4-galactan (Ebert et al., 2018; Liwanag et al., 2012). However, only *GALS1* was induced by salt stress, and the NaCl-induced accumulation of β-1,4-galactan was dependent on *GALS1* expression (Figure 3). Thus, our data are consistent with a salt-induced accumulation of β-1,4-galactan resulting from increased *GALS1* expression, which ultimately resulted in a negative effect on salt tolerance (Figures 2 and 3). Nevertheless, the endo-β-1,4-galactanase digestion (Figure 1B) and LM5 epitope detection (Figure 1D) might be affected by accessibility; we cannot exclude that there are also effects on accessibility of the β-1,4-galactans to enzymes and antibodies. The application of D-Gal, which increased β-1,4-galactan levels in *Arabidopsis*, indeed aggravated the suppression of primary root growth caused by salt stress (Rösti et al., 2007) (Figure 3 and Supplemental Figure 5). These results clearly suggest that β-1,4-galactan synthesized by GALS1 aggravates salt sensitivity.

β-1,4-Galactan served as the matrix polysaccharides entrapped by cellulose microfibrils during crystallization (Mellerowicz and Gorshkova, 2012) and trimming of β-1,4-galactan by β-1,4-galactosidase is important for final cellulose crystallization (Roach et al., 2011). Ebert et al. (2018) found that loss or accumulation of β-1,4-galactan led to minor changes in crystalline cellulose in *Arabidopsis* seedlings under normal conditions. In our study, we found that GALS1 affected the crystalline cellulose synthesis in *Arabidopsis* under salt stress (Figure 4). However, how NaCl-induced β-1,4-galactan affects crystalline cellulose synthesis is presently unclear. Sorek et al. (2015) found that the esterification levels of pectin affect cellulose synthesis, possibly by modifying the interaction of pectin and cellulose. Pectic polymers could directly tether or coat the cellulose microfibrils with neutral sugar side chains containing β-1,4-galactan (Zykwinska et al., 2007; Lin et al., 2015). It is possible that β-1,4-galactan somehow directly affects the synthesis/deposition of the cellulose at the plasma membrane in response to salt stress. Notably, β-1,4-galactan can bind to cellulose extensively and preferably, therefore limiting the access of other matrix polysaccharides, including xyloglucan, to cellulose microfibrils (Lin et al., 2015). Another possible explanation is that β-1,4-galactan induced by salt stress modulates the crystalline cellulose by altering the cellulose interaction with other matrix polysaccharides, such as xyloglucan. Moneo-Sánchez et al. (2019) showed that remodeling of β-1,4-galactan affected the degree of interaction between cellulose and xyloglucan, and the xyloglucan structure during elongation. Our previous study showed that the modified xyloglucan synthesis potentially affected crystalline cellulose synthesis in response to salt stress (Yan et al., 2019). Sustained cellulose biosynthesis was crucial for plants to maintain root growth under salt stress conditions (Zhang et al., 2016; Liu et al., 2018; Kesten et al., 2019). Based on our study and data reported previously, we present a model in which β-1,4-galactan induced by salt stress inhibits root growth by disrupting crystalline cellulose synthesis. Further studies are required to fully understand the exact mechanism of how the accumulation of β-1,4-galactan induced by salt stress disrupts cellulose synthesis in plants.

Transcriptional regulation is an important mechanism in plant response to salt stress. The transcript level of *GALS1* was significantly induced by salt stress (Figure 2); therefore, it is expected to be affected largely by transcriptional regulation. Here, we identified two transcriptional factors, BPC1 and BPC2, that directly bind to the *GALS1* promoter (Figure 5). BPC1 functions in ovule and embryo development by directly inhibiting the expression of several key transcription factors, such as *INO* (*INNER NO OUTER*), *STK* (*SEEDSTICK*), and *FUSCA3* (Meister et al., 2004; Kooiker et al., 2005; Wu et al., 2020). Class I BPCs affect the development of inflorescence meristem by suppressing the expression of *STM* (*SHOOTMERISTEMLESS*) and *BP* (*BREVIPEDICELLUS*) (Simonini and Kater, 2014). The whole members of BPC proteins directly repress *ABI4* (*ABSCISIC ACID INSENSITIVE4*) to modulate root development (Mu et al., 2017b). Here, BPC1/BPC2 repressed *GALS1* expression and the accumulation of β-1,4-galactan induced by NaCl treatment (Figure 6). Genetic analysis further showed that the salt hypersensitivity of the *bpc1-1 bpc2* double mutant was dependent on *GALS1* (Figure 7). However, the *GALS1* transcript levels and the accumulation of β-1,4-galactan in the *bpc1-1 bpc2* double mutant, the *BPC1* overexpressors, and the *BPC2* overexpressors were still clearly induced by salt stress, which implied that some other transcription factors modulating the *GALS1* transcript might exist. In addition to BPC1 and BPC2, we also screened some other transcription factors, including CBF2 and ARF2, which might directly bind to the *GALS1* promoter in yeast (Supplemental Table 2). Future work needs to identify additional candidate transcription factors in regulating *GALS1* expression in response to salt stress.

Based on these results, we propose a new regulatory mechanism by which β-1,4-galactan, regulated by the BPC1/BPC2-GALS1 module, aggravates salt sensitivity in *Arabidopsis.* When plants are under NaCl-free conditions, BPC1/BPC2 binds to the GA-rich sequence of the *GALS1* promoter and represses *GALS1* transcription to maintain a low β-1,4-galactan level with no effect on crystalline cellulose synthesis. When plants are subjected to salt stress, the transcription level of *BPC1*/*BPC2* is rapidly reduced, their suppression of *GALS1* transcription is relieved, and then synthesis of β-1,4-galactan is increased. This in turn causes disruption of the normal crystalline cellulose synthesis, and finally the plants with compromised crystalline cellulose biosynthesis show salt hypersensitivity (Figure 7E). With this mechanism in play, it is somewhat counterintuitive that *GALS1* expression is induced under salt stress, since the change leads

to increased salt sensitivity. One possibility is that the reduced growth observed under salt stress is in fact an adaptive response that ultimately improves the survival and fitness of the plants. Future studies with detailed analysis of plant response throughout the life cycle of the plant to different salt regimes will be required to fully understand the relationship between cell wall properties, root growth, and plant performance.

MATERIALS AND METHODS

Plant materials and growth conditions

Arabidopsis thaliana (L.) Heynh. Ecotype Columbia (Col-0), *gals1-1* (SALK_016687), *gals1-2* (WiscDsLox443D3), *bpc1-1* (CS68803), *bpc2* (CS68804), *bpc1-1 bpc2* (CS68700), and *prc1-1* (CS297) mutants were obtained from the Arabidopsis Biological Resource Center (ABRC). The *bpc1-1 bpc2 gals1-1* triple mutant was generated by genetic cross of the *gals1-1* single mutant and the *bpc1-1 bpc2* double mutant. The *gals1-1 prc1-1* double mutant was generated by genetic cross of the *gals1-1* single mutant and the *prc1-1* single mutant.

Seeds were sterilized and sown on solid medium containing 1/2 MS salts, including vitamins and 1% (w/v) sucrose at 4°C for 2 days, and then grown in a growth chamber (22°C, 100–200 μmol m^{-2} s^{-1}, 14 h light/10 h dark, 60% humidity).

Isolation of total RNA and real-time PCR analysis

Total RNA was isolated from plant materials using an RNAiso Plus kit (TaKaRa, China) following the manufacturer's protocol and treated with RNase-free DNase to remove contaminating DNA (TaKaRa). First-stand cDNA synthesis was performed using the iScript cDNA Synthesis Kit (Bio-Rad, USA) according to the manufacturer's protocol. Real-time PCR was performed using SYBR Premix Ex Taq (TaKaRa) according to the manufacturer's instructions. The primers used are listed in Supplemental Table 3. Expression levels for all candidate genes were determined using the $2^{-\Delta\Delta CT}$ method with *ACTIN 2* as described previously (Livak and Schmittgen, 2001).

Salt sensitivity assay

Four-day-old seedlings grown on 1/2 MS medium were transferred onto 1/2 MS medium with mannitol, salt, or various concentration of D-Gal added as described and allowed to grow for an additional 7 days. The root length was measured.

EMSA

The full-length *BPC1* and *BPC2* were amplified by PCR using the specific primers (Supplemental Table 3) and cloned into the pET30a vector. The recombinant plasmids were transformed into *E. coli* BL21 (DE3) (Navogen). His-BPC1 and His-BPC2 recombinant proteins were purified and incubated with the biotin-11-UTP-labeled DNA fragment (*GALS1* promoter oligonucleotides) for 30 min in EMSA binding buffer. The DNA signals were detected by chemiluminescence (Beyotime, China). For the competition assays, unlabeled oligonucleotides (50-fold of unlabeled probes) and labeled mutant oligonucleotides were added to the EMSA reactions.

ChIP–qPCR assay

The ChIP assay was performed as reported previously (Yan et al., 2020). *Pro-BPC1-BPC1-Myc* transgenic plants, *Pro-BPC2-BPC2-Myc* transgenic plants, anti-Myc antibodies produced in mouse (Sigma-Aldrich, USA), and Imprint Chromatin Immunoprecipitation Kit (Sigma-Aldrich) were used for ChIP experiments following the manufacturer's instructions. The enrichment of DNA fragments was quantified by qPCR using specific primers (Supplemental Table 3). A fragment of the *ACTIN 2* coding region was used as a reference gene. Enriched values were normalized with the level of input DNA.

Cell wall preparation

Four-day-old seedlings were transferred to 1/2 MS plates containing 125 mM NaCl for another 3 days. The root materials were harvested into 96% ethanol and incubated for 30 min at 100°C to inactivate cell wall-degrading enzymes. The tissue was homogenized using a Retsch MM200 mixer mill and centrifuged. The pellet was washed with 100% ethanol and twice with a mixture of chloroform and methanol (2:1), followed by four successive washes with 100% ethanol and acetone. The starch in the samples was degraded with α-amylase, amyloglucosidase, and pullulanase (Megazyme, Ireland) as described previously (Liwanag et al., 2012). The pellet was air-dried overnight and was referred to as AIR (alcohol-insoluble residue).

Cell wall fractionation and composition analyses

Pectic polysaccharides were extracted from AIR by combining three hot water extracts at 100°C for 1 h each. Subsequently, hemicellulose polysaccharides were extracted by treating the remaining pellet three times with 4% (w/v) KOH containing 0.02% (w/v) $NaBH_4$ at 25°C for 12 h. The uronic acid content in the pectic polysaccharides was determined by M-hydroxy-diphenyl assay (Blumenkrantz and Asboe-Hansen, 1973). The total polysaccharide content in the hemicellulose fraction was determined using the phenol sulfuric acid method (Dubois et al., 1956).

About 2 mg of AIR was hydrolyzed in 2 M TFA at 121°C for 1 h. The insoluble material was further hydrolyzed with Updegraff reagent at 100°C for 30 min. Then, the crystalline cellulose content was quantified by the anthrone assay (Updegraff, 1969).

Analysis of cell wall monosaccharide composition

Dried AIR (2 mg) was hydrolyzed in 2 M TFA at 121°C for 1 h, and analyzed by high-performance anion exchange chromatography (HPAEC) on an ICS-5000 instrument (Thermo Fisher Scientific, USA) equipped with a CarboPac PA20 (3 × 150 mm, Thermo Fisher Scientific) analytical anion exchange column, PA20 guard column (3 × 30 mm), borate trap, and a pulsed amperometric detector.

AIR was further analyzed by digestion with endo-β-1,4-galactanase from *Aspergillus niger* (Megazyme) according to (Liwanag et al., 2012). AIR (2 mg) was dissolved in 0.1 ml of 1 M KOH and adjusted to pH 4.7 with acetic acid. Two units of galactanase were added and incubated for 1 h at 40°C. Then, cold 95% ethanol with 10 mM EDTA was added to a final concentration of 70% and the sample was centrifuged at 14 000 × *g* for 5 min at 4°C. The supernatant and pellet were separated, dried, hydrolyzed with 2 M TFA, and analyzed by HPAEC to measure the D-Gal content.

Immunodot assays

Immunodot assays were performed as described previously (Liwanag et al., 2012). In brief, 2 mg AIR, potato galactan, and sugar beet pectin were treated with 2:1:1 (v/v/v) phenol:acetic acid:water to remove soluble proteins. Then, the above samples were extracted with 4 M KOH containing 0.1% $NaBH_4$. Dilution of the extracts was spotted onto nitrocellulose, then the nitrocellulose was blocked with 5% milk powder in phosphate-buffered saline (PBS) buffer for 30 min. The nitrocellulose was incubated with a 10-fold dilution of LM5 or LM19 (PlantProbes, UK) for 1 h. The primary antibody was thoroughly washed off the samples with PBS three times. Next, the samples were incubated with a 2000-fold dilution of secondary antibody (goat anti-rat IgG coupled with horseradish peroxidase, Sigma-Aldrich) for 1 h. A camera (Takon 5200 Multi, Tanon Biomart, China) was used to capture the signal. Potato galactan or sugar beet pectin (Megazyme) was used as positive control and water was used as a negative control. Quantification was done using ImageJ software. The control (bottom left) intensity in each nitrocellulose membrane was set to 100 and others were compared with it.

Indirect immunofluorescence

Indirect immunofluorescence was done according to Geng et al. (2017). In brief, roots were fixed in 2.5% glutaraldehyde in 0.2 M sodium PBS (pH 7.0) for 1–2 h, then the samples were washed three times with PBS and blocked with 0.2% BSA in PBS buffer for 0.5 h. The samples were incubated with a 10-fold dilution of LM5 (PlantProbes) for 1 h. The LM5 antibody was thoroughly washed off the samples with PBS three times. Next, the samples were incubated with a 100-fold dilution of secondary antibody (Alexa Fluor 555-labeled donkey anti-rat IgG, Abcam, UK) for 1 h. A solution of 5 μg/ml DAPI (Beyotime) in PBS buffer was added for 20 min to stain the nucleus. The samples were washed as mentioned above, mounted on glass slides, and examined under a Leica laser-scanning confocal microscope with an excitation at 555 nm and emission at 564–594 nm (for LM5) or an excitation at 360 nm and emission at 466 nm (for DAPI) (Leica, TCP SP8, Germany).

S4B staining

Roots were fixed in 2.5% glutaraldehyde in 0.2 M sodium PBS (pH 7.0) for 1–2 h, followed by staining with 0.01% S4B (Sigma-Aldrich). A solution of 5 μg/ml DAPI (Beyotime) in PBS buffer was added for 20 min to stain the nucleus. Images were taken using the Leica laser-scanning confocal microscope with an excitation at 543 nm and emission at 585–615 nm (for S4B) or an excitation at 360 nm and emission at 466 nm (for DAPI) (Leica, TCP SP8).

Quantification of fluorescence signals

LM5, S4B, and DAPI signal areas were measured with ImageJ software (Silva-Sanzana et al., 2019). Each image was transformed to a 16-bit image, and the threshold was adjusted for each channel (LM5, S4B, and DAPI) using the same threshold parameters for all replicates. The areas in the root tip (about 500 μm) were separated with the option "Polygon selections." The fluorescence signal (LM5, S4B, and DAPI) was separately measured with the menu tool "measure." Then, the relative intensity of LM5 or S4B fluorescence was calculated by dividing the LM5 or S4B signal by the DAPI signal. The pseudo-color image representing the fluorescence intensity (LM5 and S4B) was also converted by ImageJ software. Image was transformed to a 16-bit image. Then, the pseudo-color image was obtained with the option "Lookup Tables (16 colors)." The color scales below the figures indicate the fluorescence intensity.

ACCESSION NUMBER

Sequence data from this article can be found in the Arabidopsis Genome Initiative database under accession numbers: *ACTIN 2* (AT3G18780), *GALS1* (AT2G33570), *GALS2* (AT5G44670), *GALS3* (AT4G20170), *CESA6* (AT5G64740), *BPC1* (AT2G01930), *BPC2* (AT1G14685), and *BPC3* (AT1G68120). The raw data of the RNA sequencing have been submitted to the NCBI Sequence Read Archive database under accession number PRJNA668243.

SUPPLEMENTAL INFORMATION

Supplemental Information is available at *Molecular Plant Online*.

FUNDING

This study was supported by grants from the National Natural Science Foundation of China (31871534 and 32001445); the Natural Science Foundation of Jiangsu Province (BK20200557); the China Postdoctoral Science Foundation (2019M651846); the Six Talent Peaks Program of Jiangsu Province (2016-NY-079); and the Natural Science Foundation of Guangdong Province (2018A030313686). H.V.S. was supported through the Joint BioEnergy Institute (http://www.jbei.org) by the U.S. Department of Energy, Office of Science, Office of Biological and Environmental Research, through contract DE-AC02-05CH11231 between Lawrence Berkeley National Laboratory and the U.S. Department of Energy.

AUTHOR CONTRIBUTIONS

A.Z. and J.Y. conceived the project and designed the experiments. J.Y. performed most of the experiments and analyzed the data. J.Y. and A.Z. wrote the manuscript. Y.L. performed the indirect immunofluorescence. Y.L., L.Y., H.H., and Y.H. generated the transgenic lines. L.F., H.V.S., and M.J. revised the manuscript.

ACKNOWLEDGMENTS

We are grateful to ABRC at Ohio State University for providing *Arabidopsis* seed stock. No conflict of interest declared.

Received: June 7, 2020
Revised: October 12, 2020
Accepted: November 30, 2020
Published: December 1, 2020

REFERENCES

Anderson, C.T., Carroll, A., Akhmetova, L., and Somerville, C. (2010). Real-time imaging of cellulose reorientation during cell wall expansion in *Arabidopsis* roots. Plant Physiol. **152**:787–796.

Atmodjo, M.A., Hao, Z., and Mohnen, D. (2013). Evolving views of pectin biosynthesis. Annu. Rev. Plant Biol. **64**:747–779.

Blumenkrantz, N., and Asboe-Hansen, G. (1973). New method for quantitative determination of uronic acids. Anal. Biochem. **54**:484–489.

Chen, Z., Hong, X., Zhang, H., Wang, Y., Li, X., Zhu, J.K., and Gong, Z. (2005). Disruption of the cellulose synthase gene, AtCesA8/IRX1, enhances drought and osmotic stress tolerance in *Arabidopsis*. Plant J. **43**:273–283.

Cosgrove, D.J. (2015). Plant expansins: diversity and interactions with plant cell walls. Curr. Opin. Plant Biol. **25**:162–172.

Dörmann, P., and Benning, C. (1998). The role of UDP-glucose epimerase in carbohydrate metabolism of *Arabidopsis*. Plant J. **13**:641–652.

Dubois, M., Gilles, K.A., Hamilton, J.K., Rebers, P.t., and Smith, F. (1956). Colorimetric method for determination of sugars and related substances. Anal. Chem. **28**:350–356.

Ebert, B., Birdseye, D., Liwanag, A.J., Laursen, T., Rennie, E.A., Guo, X., Catena, M., Rautengarten, C., Stonebloom, S.H., Gluza, P., et al. (2018). The three members of the *Arabidopsis* glycosyltransferase family 92 are functional β-1,4-galactan synthases. Plant Cell Physiol. **59**:2624–2636.

Endler, A., Kesten, C., Schneider, R., Zhang, Y., Ivakov, A., Froehlich, A., Funke, N., and Persson, S. (2015). A mechanism for sustained cellulose synthesis during salt stress. Cell **162**:1353–1364.

Fagard, M., Desnos, T., Desprez, T., Goubet, F., Refregier, G., Mouille, G., McCann, M., Rayon, C., Vernhettes, S., and Höfte, H. (2000). PROCUSTE1 encodes a cellulose synthase required for normal cell elongation specifically in roots and dark-grown hypocotyls of *Arabidopsis*. Plant Cell **12**:2409–2423.

Galvan-Ampudia, C.S., and Testerink, C. (2011). Salt stress signals shape the plant root. Curr. Opin. Plant Biol. **14**:296–302.

Geng, X., Horst, W.J., Golz, J.F., Lee, J.E., Ding, Z., and Yang, Z.B. (2017). LEUNIG_HOMOLOG transcriptional co-repressor mediates aluminium sensitivity through PECTIN METHYLESTERASE46-modulated root cell wall pectin methylesterification in *Arabidopsis*. Plant J. **90**:491–504.

Ha, M.A., Viëtor, R.J., Jardine, G.D., Apperley, D.C., and Jarvis, M.C. (2005). Conformation and mobility of the arabinan and galactan side-chains of pectin. Phytochemistry **66**:1817–1824.

Harholt, J., Suttangkakul, A., and Scheller, H.V. (2010). Biosynthesis of pectin. Plant Physiol. **153**:384–395.

Herburger, K., Franková, L., Pičmanová, M., Loh, J.W., Valenzuela-Ortega, M., Meulewaeter, F., Hudson, A., French, C.E., and Fry, S.C. (2020). Hetero-trans-β-glucanase produces cellulose-xyloglucan covalent bonds in the cell walls of structural plant tissues and is stimulated by expansin. Mol. Plant **13**:1–16.

Jones, L., Seymour, G.B., and Knox, J.P. (1997). Localization of pectic galactan in tomato cell walls using a monoclonal antibody specific to (1[→] 4)-[beta]-D-galactan. Plant Physiol. **113**:1405–1412.

Julkowska, M.M., and Testerink, C. (2015). Tuning plant signaling and growth to survive salt. Trends Plant Sci. **20**:586–594.

Kang, J.S., Frank, J., Kang, C.H., Kajiura, H., Vikram, M., Ueda, A., Kim, S., Bahk, J.D., Triplett, B., Fujiyama, K., et al. (2008). Salt tolerance of *Arabidopsis thaliana* requires maturation of N-glycosylated proteins in the Golgi apparatus. Proc. Natl. Acad. Sci. U S A **105**:5933–5938.

Kesten, C., Wallmann, A., Schneider, R., McFarlane, H.E., Diehl, A., Khan, G.A., van Rossum, B.-J., Lampugnani, E.R., Szymanski, W.G., Cremer, N., et al. (2019). The companion of cellulose synthase 1 confers salt tolerance through a Tau-like mechanism in plants. Nat. Commun. **10**:1–14.

Kooiker, M., Airoldi, C.A., Losa, A., Manzotti, P.S., Finzi, L., Kater, M.M., and Colombo, L. (2005). BASIC PENTACYSTEINE1, a GA binding protein that induces conformational changes in the regulatory region of the homeotic *Arabidopsis* gene SEEDSTICK. Plant Cell **17**:722–729.

Laursen, T., Stonebloom, S.H., Pidatala, V.R., Birdseye, D.S., Clausen, M.H., Mortimer, J.C., and Scheller, H.V. (2018). Bifunctional glycosyltransferases catalyze both extension and termination of pectic galactan oligosaccharides. Plant J. **94**:340–351.

Lin, D., Lopez-Sanchez, P., and Gidley, M.J. (2015). Binding of arabinan or galactan during cellulose synthesis is extensive and reversible. Carbohyd. Polym. **126**:108–121.

Liu, C., Niu, G., Zhang, H., Sun, Y., Sun, S., Yu, F., Lu, S., Yang, Y., Li, J., and Hong, Z. (2018). Trimming of N-glycans by the Golgi-localized α-1,2-mannosidases, MNS1 and MNS2, is crucial for maintaining RSW2 protein abundance during salt stress in *Arabidopsis*. Mol. Plant **11**:678–690.

Livak, K.J., and Schmittgen, T.D. (2001). Analysis of relative gene expression data using real-time quantitative PCR and the $2^{-\Delta\Delta CT}$ method. Methods **25**:402–408.

Liwanag, A.J.M., Ebert, B., Verhertbruggen, Y., Rennie, E.A., Rautengarten, C., Oikawa, A., Andersen, M.C., Clausen, M.H., and Scheller, H.V. (2012). Pectin biosynthesis: GALS1 in *Arabidopsis thaliana* is a β-1,4-galactan β-1,4-galactosyltransferase. Plant Cell **24**:5024–5036.

McCartney, L., Steele-King, C.G., Jordan, E., and Knox, J.P. (2003). Cell wall pectic (1→4)-β-D-galactan marks the acceleration of cell elongation in the *Arabidopsis* seedling root meristem. Plant J. **33**:447–454.

Meister, R.J., Williams, L.A., Monfared, M.M., Gallagher, T.L., Kraft, E.A., Nelson, C.G., and Gasser, C.S. (2004). Definition and interactions of a positive regulatory element of the *Arabidopsis* INNER NO OUTER promoter. Plant J. **37**:426–438.

Mellerowicz, E.J., and Gorshkova, T.A. (2012). Tensional stress generation in gelatinous fibres: a review and possible mechanism based on cell-wall structure and composition. J. Exp. Bot. **63**:551–565.

Moneo-Sánchez, M., Alonso-Chico, A., Knox, J.P., Dopico, B., Labrador, E., and Martín, I. (2019). β-(1,4)-Galactan remodelling in *Arabidopsis* cell walls affects the xyloglucan structure during elongation. Planta **249**:351–362.

Monfared, M.M., Simon, M.K., Meister, R.J., Roig-Villanova, I., Kooiker, M., Colombo, L., Fletcher, J.C., and Gasser, C.S. (2011). Overlapping and antagonistic activities of BASIC PENTACYSTEINE genes affect a range of developmental processes in *Arabidopsis*. Plant J. **66**:1020–1031.

Mu, Y., Liu, Y., Bai, L., Li, S., He, C., Yan, Y., Yu, X., and Li, Y. (2017a). Cucumber CsBPCs regulate the expression of CsABI3 during seed germination. Front. Plant Sci. **8**:459.

Mu, Y., Zou, M., Sun, X., He, B., Xu, X., Liu, Y., Zhang, L., and Chi, W. (2017b). BASIC PENTACYSTEINE proteins repress ABSCISIC ACID INSENSITIVE4 expression via direct recruitment of the polycomb-repressive complex 2 in *Arabidopsis* root development. Plant Cell Physiol. **58**:607–621.

Munns, R., and Tester, M. (2008). Mechanisms of salinity tolerance. Annu. Rev. Plant Biol. **59**:651–681.

Mutwil, M., Debolt, S., and Persson, S. (2008). Cellulose synthesis: a complex complex. Curr. Opin. Plant Biol. **11**:252–257.

Øbro, J., Borkhardt, B., Harholt, J., Skjøt, M., Willats, W.G., and Ulvskov, P. (2009). Simultaneous in vivo truncation of pectic side chains. Transgenic Res. **18**:961–969.

Rösti, J., Barton, C.J., Albrecht, S., Dupree, P., Pauly, M., Findlay, K., Roberts, K., and Seifert, G.J. (2007). UDP-glucose 4-epimerase isoforms UGE2 and UGE4 cooperate in providing UDP-galactose for cell wall biosynthesis and growth of *Arabidopsis thaliana*. Plant Cell **19**:1565–1579.

Roach, M.J., Mokshina, N.Y., Badhan, A., Snegireva, A.V., Hobson, N., Deyholos, M.K., and Gorshkova, T.A. (2011). Development of cellulosic secondary walls in flax fibers requires β-galactosidase. Plant Physiol. **156**:1351–1363.

Sangwan, I., and O'Brian, M.R. (2002). Identification of a soybean protein that interacts with GAGA element dinucleotide repeat DNA. Plant Physiol. **129**:1788–1794.

Santi, L., Wang, Y., Stile, M.R., Berendzen, K., Wanke, D., Roig, C., Pozzi, C., Müller, K., Müller, J., Rohde, W., et al. (2003). The GA octodinucleotide repeat binding factor BBR participates in the transcriptional regulation of the homeobox gene Bkn3. Plant J. **34**:813–826.

Scheller, H.V., and Ulvskov, P. (2010). Hemicelluloses. Annu. Rev. Plant Biol. **61**:263–289.

Seifert, G.J., Barber, C., Wells, B., Dolan, L., and Roberts, K. (2002). Galactose biosynthesis in *Arabidopsis*: genetic evidence for substrate channeling from UDP-D-galactose into cell wall polymers. Curr. Biol. **12**:1840–1845.

Shanks, C.M., Hecker, A., Cheng, C.Y., Brand, L., Collani, S., Schmid, M., Schaller, G.E., Wanke, D., Harter, K., and Kieber, J.J. (2018). Role of BASIC PENTACYSTEINE transcription factors in a subset of cytokinin signaling responses. Plant J. **95**:458–473.

Silva-Sanzana, C., Celiz-Balboa, J., Garzo, E., Marcus, S.E., Parra-Rojas, J.P., Rojas, B., Olmedo, P., Rubilar, M.A., Rios, I., Chorbadjian, R.A., et al. (2019). Pectin methylesterases modulate plant homogalacturonan status in defenses against the aphid *Myzus persicae*. Plant Cell **31**:1913–1929.

Simonini, S., and Kater, M.M. (2014). Class I BASIC PENTACYSTEINE factors regulate HOMEOBOX genes involved in meristem size maintenance. J. Exp. Bot. **65**:1455–1465.

Simonini, S., Roig-Villanova, I., Gregis, V., Colombo, B., Colombo, L., and Kater, M.M. (2012). Basic pentacysteine proteins mediate MADS domain complex binding to the DNA for tissue-specific expression of target genes in *Arabidopsis*. Plant Cell **24**:4163–4172.

Sorek, N., Szemenyei, H., Sorek, H., Landers, A., Knight, H., Bauer, S., Wemmer, D.E., and Somerville, C.R. (2015). Identification of MEDIATOR16 as the *Arabidopsis* COBRA suppressor MONGOOSE1. Proc. Natl. Acad. Sci. U S A **112**:16048–16053.

Stonebloom, S., Ebert, B., Xiong, G., Pattathil, S., Birdseye, D., Lao, J., Pauly, M., Hahn, M.G., Heazlewood, J.L., and Scheller, H.V. (2016). A DUF-246 family glycosyltransferase-like gene affects male fertility and the biosynthesis of pectic arabinogalactans. BMC Plant Biol. **16**:90.

Tang, H., Belton, P.S., Ng, A., and Ryden, P. (1999). ^{13}C MAS NMR studies of the effects of hydration on the cell walls of potatoes and Chinese water chestnuts. J. Agric. Food Chem. **47**:510–517.

Tenhaken, R. (2015). Cell wall remodeling under abiotic stress. Front. Plant Sci. **5**:771.

Ulvskov, P., Wium, H., Bruce, D., Jørgensen, B., Qvist, K.B., Skjøt, M., Hepworth, D., Borkhardt, B., and Sørensen, S.O. (2005). Biophysical consequences of remodeling the neutral side chains of rhamnogalacturonan I in tubers of transgenic potatoes. Planta **220**:609–620.

Updegraff, D.M. (1969). Semimicro determination of cellulose inbiological materials. Anal. Biochem. **32**:420–424.

Verhertbruggen, Y., Walker, J.L., Guillon, F., and Scheller, H.V. (2017). A comparative study of sample preparation for staining and immunodetection of plant cell walls by light microscopy. Front. Plant Sci. **8**:1505.

Verhertbruggen, Y., Marcus, S.E., Haeger, A., Ordaz-Ortiz, J.J., and Knox, J.P. (2009). An extended set of monoclonal antibodies to pectic homogalacturonan. Carbohyd. Res. **344**:1858–1862.

Wang, T., McFarlane, H.E., and Persson, S. (2016). The impact of abiotic factors on cellulose synthesis. J. Exp. Bot. **67**:543–552.

Wu, J., Mohamed, D., Dowhanik, S., Petrella, R., Gregis, V., Li, J.R., Wu, L., and Gazzarrini, S. (2020). Spatiotemporal restriction of FUSCA3 expression by class I BPCs promotes ovule development and coordinates embryo and endosperm growth. Plant Cell **32**:1886–1904.

Yan, J., Fang, L., Yang, L., He, H., Huang, Y., Liu, Y., and Zhang, A. (2020). Abscisic acid positively regulates L-arabinose metabolism to inhibit seed germination through ABSCISIC ACID INSENSITIVE4-mediated transcriptional promotions of MUR4 in *Arabidopsis thaliana*. New Phytol. **225**:823–834.

Yan, J., Huang, Y., He, H., Han, T., Di, P., Sechet, J., Fang, L., Liang, Y., Scheller, H.V., Mortimer, J.C., et al. (2019). Xyloglucan endotransglucosylase-hydrolase30 negatively affects salt tolerance in *Arabidopsis*. J. Exp. Bot. **70**:5495–5506.

Yan, T., Yoo, D., Berardini, T.Z., Mueller, L.A., Weems, D.C., Weng, S., Cherry, J.M., and Rhee, S.Y. (2005). PatMatch: a program for finding patterns in peptide and nucleotide sequences. Nucleic Acids Res. **33**:W262–W266.

Zhang, S.S., Sun, L., Dong, X., Lu, S.J., Tian, W., and Liu, J.X. (2016). Cellulose synthesis genes CESA6 and CSI1 are important for salt stress tolerance in *Arabidopsis*. J. Integr. Plant Biol. **58**:623–626.

Zhu, J., Lee, B.H., Dellinger, M., Cui, X., Zhang, C., Wu, S., Nothnagel, E.A., and Zhu, J.K. (2010). A cellulose synthase-like protein is required for osmotic stress tolerance in *Arabidopsis*. Plant J. **63**:128–140.

Zhu, J.K. (2002). Salt and drought stress signal transduction in plants. Annu. Rev. Plant Biol. **53**:247–273.

Zhu, J.K. (2016). Abiotic stress signaling and responses in plants. Cell **167**:313–324.

Zykwinska, A., Thibault, J.F., and Ralet, M.C. (2007). Organization of pectic arabinan and galactan side chains in association with cellulose microfibrils in primary cell walls and related models envisaged. J. Exp. Bot. **58**:1795–1802.